Simulating human photoreceptor optics using a liquid-filled photonic crystal fiber

Diego Rativa[1,*] **and Brian Vohnsen**[1]

[1]*Advanced Optical Imaging Group School of Physics, University College Dublin, Dublin 4, Ireland*

**diego-jose.rativa-millan@ucd.ie*

Abstract: We introduce a liquid-filled photonic crystal fiber to simulate a retinal cone photoreceptor mosaic and the directionality selective mechanism broadly known as the Stiles-Crawford effect. Experimental measurements are realized across the visible spectrum to study waveguide coupling and directionality at different managed waveguide parameters. The crystal fiber method is a hybrid tool between theory and a real biological sample and a valuable addition as a retina model for real eye simulations.

OCIS codes: (330.7331) Visual optics, receptor optics; (330.7326) Visual optics, modeling; (060.5295) Photonic crystal fibers.

References and links

1. C. A. Curcio, K. R. Sloan, R. E. Kalina, and A. E. Hendrickson, "Human photoreceptor topography," J. Comp. Neurol. **292**, 497–523 (1990).
2. G. Toraldo di Francia, "Retina cones as dielectric antennas," J. Opt. Soc. Am. **39,** 324–324 (1949).
3. J. M. Enoch, "Waveguide modes: Are they present, and what is their possible role in the visual mechanism?" J. Opt. Soc. Am. **50,** 1025–1026 (1960).
4. J. M. Enoch, "Optical properties of the retinal receptors," J. Opt. Soc. Am. **53,** 71–85 (1963).
5. S. Marcos, S. A. Burns, and J. C. He, "Model for cone directionality reflectometric measurements based on scattering," J. Opt. Soc. Am. A **15,** 2012–2022 (1998).
6. N. P. Zagers, T. T. J. M. Berendschot, J. van de Kraats, and D. van Norren, "Wavelength dependence of reflectometric cone photoreceptor directionality," J. Opt. Soc. Am. A **20,** 18–23 (2003).
7. T. T. J. M. Berendschot, J. van de Kraats, and D. van Norren, "Wavelength dependence of the Stiles-Crawford effect explained by perception of backscattered light from the choroid," J. Opt. Soc. Am. A **18,** 1445–1451 (2003).
8. A. W. Snyder and C. Pask, "The Stiles-Crawford effect explanation and consequences," Vision Res. **13,** 1115–1137 (1973).
9. B. Vohnsen, I. Iglesias, and P. Artal, "Guided light and diffraction model of human-eye photoreceptors," J. Opt. Soc. Am. A **22,** 2318–2328 (2005).
10. W. S. Stiles, "The directional sensitivity of the retina and the spectral sensitivities of the rods and cones," Proc. R. Soc., London, Ser. B **127**, 64–105 (1939).
11. V. Lakshminarayanan and J. M. Enoch, "Biological waveguides," in Handbook of Optics Vol. III, 2nd ed., M. Bass, ed. (McGraw-Hill, 2001), Chap. 9.
12. G. Westheimer, "Directional sensitivity of the retina: 75 years of Stiles-Crawford effect," Proc. R. Soc., London, Ser. B **275**, 2777–2786 (2008).
13. J. M. Enoch and G. A. Fry, "Characteristics of a model retinal receptor studied at microwave frequencies," J. Opt. Soc. Am. **48,** 899–910 (1958).
14. J. Limeres, M. L. Calvo, J. M. Enoch, and V. Lakshminarayana, "Light scattering by an array of birefringent optical waveguides: theoretical foundations," J. Opt. Soc. Am. B **20,** 1542–1549 (2003).
15. B. Vohnsen, "On the spectral relation between the first and second Stiles-Crawford effect," J. Mod. Opt. **56**, 2261–2271 (2009).
16. P. St. J. Russell, "Photonic crystal fibers," Science **299**, 358–362 (2003).
17. J. C. Knight, "Photonic crystal fibers," Nature **424**, 847–851 (2003).

#135685 - $15.00 USD Received 28 Sep 2010; revised 3 Dec 2010; accepted 26 Jan 2011; published 11 Feb 2011

18. C. R. Rosberg, F. H. Bennet, D. N. Neshev, P. D. Rasmussen, O. Bang, W. Krolikowski, A. Bjarklev, and Y. S. Kivshar, "Tunable diffraction and self-defocusing in liquid-filled photonic crystal fibers," Opt. Express **15,** 12145–12150 (2007).
19. I. Malitson, "Interspecimen comparison of the refractive index of fused silica," J. Opt. Soc. Am. **55,** 1205–1209 (1965).
20. K. Nikolova, I. Panchev, and S. Sainov, "Optical characteristics of oil, obtained from sea-buckthorn," Eur. Food Res. Technol. **223**, 843–847 (2006).
21. R. F. Souza, M. A. Alencar, M. Meneghetti, and J. Hickmann, "Large nonlocal nonlinear optical response of castor oil," Opt. Mat. **31**, 1591–1594 (2009).
22. L. Rindorf, P. E. Hoiby, J. B. Jensen, L. H. Pedersen, O. Bang, and O. Geschke, "Biomolecule detection with integrated evanescent-wave microstructured optical fibre sensor," Anal. Bioanal. Chem., 1–6 (2006).
23. Z. Hui, Z. Guiliang, and D. Wang, "Super-Gaussian window function and its applications," in *Circuits and Systems, Conference Proceedings China, Shenzhen, 1991*, pp. 595–598.
24. J. M. Enoch and G. M. Hope, "Directional sensitivity of the foveal and parafoveal retina," Invest. Ophthalmol. Visual Sci. **12**, 497–503 (1973).
25. N. Lue, W. Choi, G. Popescu, Z. Yaqoob, K. Badizadegan, R. R. Dasari, and M. S. Feld, "Live cell refractometry using Hilbert phase microscopy and confocal reflectance microscopy," J. Phys. Chem. A **113**, 13327–13330 (2009).
26. B. Vohnsen, "Photoreceptor waveguides and effective retinal image quality," J. Opt. Soc. Am. A **24,** 597–607 (2007).
27. R. Barer, "Refractometry and interferometry of living cells," J. Opt. Soc. Am. **47,** 545–556 (1957).
28. R. Sidman, "The structure and concentration of solids in photoreceptor cells studied by refractometry and interference microscopy," J. Biophys. Biochem. Cytol. **3** 15–30 (1957).

1. Introduction

The photoreceptors are organized in a highly ordered array in the human retina. At the fovea the densely packed cones resemble rods with diameters (d_i) between 2-3μm separated by an intercone distance of 2-3μm, whereas at the parafoveal region the cones are more conical with diameters ranging between 5-8μm and are less densely packed [1]. Toraldo di Francia (1949) drew attention to the similarity between waveguides and retinal photoreceptors, and the possibility to explain the Stiles-Crawford effect (SCE) as being due to the directionality selective mechanism of the waveguides [2], but only in the 1960's were the first observations of waveguide mode patterns in photoreceptors reported by Enoch [3,4], and thus providing evidence that the retina is a microstructure whose cones work as waveguides of light from the inner to the outer cone segments.

In general two approaches dominate when explaining the directionality mechanism and its wavelength dependence throughout the visible spectrum. One approach is based on the backscattering effects created by the waveguide properties of the cones and the topography of the cone mosaic [5]. The approach is in agreement with the wavelength dependence of the Optical Stiles-Crawford (OSCE) [6]. A related approach has been used to describe the directionality of the SCE as being due to backscattering of light from the choroid [7].

Another approach based on the Enoch's observation of mode patterns in retinal receptors [4] has been formulated by Snyder and Pask [8]. The model assumes that the SCE is created by the light-coupling mechanism to discrete waveguide modes of the cones. The coupling and the consequences in the apodization effect at the pupil are highly sensitive to the waveguide parameter V, defined as $V = (\pi d_i/\lambda)NA$, where λ is the wavelength of the light propagated, and d_i and NA is the size and the numerical aperture of a given individual photoreceptor, respectively. Recently, B. Vohnsen et al. [9] have upgraded the Snyder and Pask model to include the diffraction properties of the light to/from the pupil obtaining analytical expressions for the directionality parameters in agreement with the OSCE and SCE results [6, 10].

However, due to the difficulties of the biological preparation as well as real-eye measurements, the theoretical models are considered abstractions and the formulations quite simplistic for the complex mechanism of the eye and vision [11, 12]. One step towards filling the gap

#135685 - $15.00 USD Received 28 Sep 2010; revised 3 Dec 2010; accepted 26 Jan 2011; published 11 Feb 2011

between the theoretical models and a retinal tissue is to simulate the biological structure with experimental devices such that a hybrid situation between theory and experiment is created enabling precise control of its characteristics. To our knowledge, such an approach has only been previously attempted using a large-scale microwave guiding cylindrical structure [13]. Related theoretical approaches have previously been developed to examine scattering by fiber-optic bundles [14], but here the analysis will be based on uncoupled photoreceptor waveguides that suffice to reproduce the overall appearance of the experimentally reported SCE directionality [15].

The photonic crystal fiber (PCF) is a silica waveguide (optimized for visible and near-infrared light) with a microstructure of air holes extended along the fiber to localize guiding to its core [16]. In a variation usually named as the liquid-filled photonic crystal fiber (LF-PCF) high-refractive liquids are used to fill the air holes, hence the light is guided by the liquid-filled holes instead [17]. Rosberg, et al. [18] have used Castor oil which has a high negative thermo-optical coefficient, under these conditions the light is guided by the liquid in the holes and the waveguide properties are accurately managed by temperature control. Therefore, the LF-PCF works as a micrometric fiber bundle [Fig. 2(a)], whose waveguide characteristics (single- and multimode) are well-controlled by changing the index of refraction of the infiltrated liquid.

In this work we have used an optical setup with a lens imitating the refractive human eye and the LF-PCF imitating the retina. Simulated Stiles-Crawford (SSC) measurements have been performed measuring the transmitted light power through the LF-PCF to study coupling and directionality for different waveguide conditions, i.e. V$\propto$NA (λ=constant) and V$\propto 1/\lambda$ (NA=constant). Both the SCE and OSCE situations are experimentally simulated considering the model of diffraction to/from the pupil and considering the subjective SCE visibility to be proportional to the coupled light power [9].

2. Experimental measurements

2.1. Set-up

As shown in Fig. 1(b) a lens (L_1) (f=25mm, achromatic, 1/2" Ø) is used as the simulated refractive eye focusing the light at the plane where the LF-PCF is located. The LF-PCF is implemented using a commercially available photonic Crystal Fiber (LMA-20, 30mm long, optimized operation for the near-infrared region) and the air holes are filled with Castor Oil by use of capillary forces [18]. The LMA-20 fiber has air holes with diameter of 6.4μm separated by a distance of 13.2μm [Fig. 2(b)]. Therefore, for the LF-PCF method, the inter-waveguide and waveguide size should be compared to the cone size and the inter-cone distance of the retina.

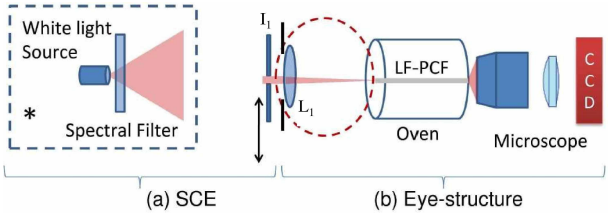

Fig. 1. Experimental setup: (a) Illumination for SCE measurements (* not to scale), (b) optical setup.

The LF-PCF is placed inside of a precision oven (Oven & Tec, Caston Inc.) with a resolution of $\pm 0.1^{\circ}$C, allowing accurate thermal control of its refractive properties. A lapse time of 10min for thermal stabilization is used for each new temperature set point prior to measurements. The lens and the oven are mounted in a vertical position in an Olympus Microscope (BX61, 20X

#135685 - $15.00 USD Received 28 Sep 2010; revised 3 Dec 2010; accepted 26 Jan 2011; published 11 Feb 2011

objective), after propagation through the LF-PCF the guided light is imaged by the objective onto the CCD camera. A thin glass plate ($n_{glass} = 1.5$) is in optical contact with the entry face of the LF-PCF to avoid oil spilling.

2.2. *Simulated Stiles-Crawford method*

A fiber-based white light tungsten-halogen source was used as illumination source. The nominal source width at the fiber-bundle exit is 5.4mm. A kit of spectral filters from 450nm to 670nm (each one with a 10nm bandpass) was used to select the wavelength of illumination. The optical setup with a lens imitating the refractive human eye and the LF-PCF imitating the retina is located at a distance of 2m from the light source such that the illumination is approximately collimated at the pupil area of the lens. As shown in Fig. 2(a) and 2(b), the light is focused at a small region of the LF-PCF ($\sim$30 holes), reducing as much as possible the residual light guided by the central part of the crystal fiber. The SSC experiment consists of scanning the pupil plane by using a moveable iris (I_1) with diameter of 0.8mm and to measure the average fraction of light guided by the oil-filled holes. Only the fraction of power within each oil-filled hole is included in our measurements and this value is averaged for all holes included in the illuminated area. Only the light guided by the LF-PCF (30mm) is detected by the CCD camera, ruling out possible scattering influences from the coupling face.

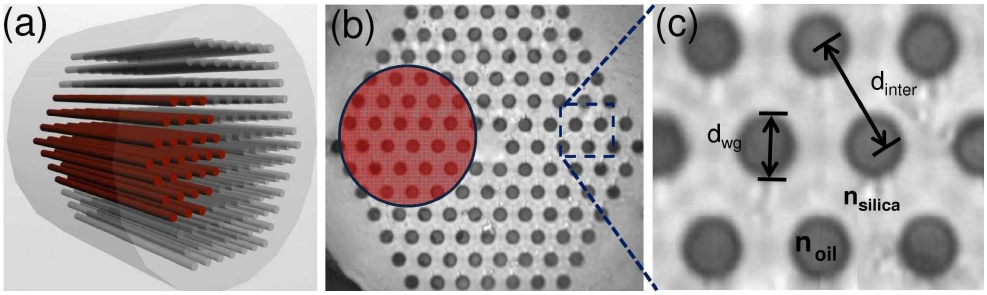

Fig. 2. LF-PCF fiber bundle: (a-b) region used for the SSC measurements (red), and (b-c) section of fiber cladding (LMA-20: d_{inter} = 13.2μm and d_{wg} = 6.4μm) where n_{silica} and $n_{oil}(T)$ are the indices of refraction of Silica and Castor Oil (managed by temperature), respectively).

2.3. *Thermo-optical coefficients*

A refined control of the refractive properties is necessary to manage the waveguide V-number and thus the modes coupled to the waveguide. Taking into account the Sellmeier curves for Silica at 20°C [19], and assuming a Castor Oil dispersion approximated by similar vegetal oils at 18°C [20], it is possible to estimate the thermo-optical coefficients of the Castor Oil (K^{oil}) between 450-670nm. To this end, we measure the temperature at which the light guiding capability by the filled holes is lost, i.e., when the Silica and the Castor Oil have the same indices of refraction ($n_{silica}(\lambda) = n_{oil}(\lambda)$). The thermo-optical coefficients calculated are in the range between $K^{oil}_{(450nm)}$ =-4.7$\pm$0.1$\times10^{-4\circ}C^{-1}$ and $K^{oil}_{(670nm)}$ =-2.7$\pm$0.1$\times10^{-4\circ}C^{-1}$ in agreement with previously reported values at 532*nm* [18, 21]. The thermo-optical effect of the Silica has been neglected because its thermo-optical coefficient is within the K^{oil} standard deviation (K^{silica} =-1.2$\times10^{-5}$ $^{\circ}C^{-1}$) [22].

#135685 - $15.00 USD Received 28 Sep 2010; revised 3 Dec 2010; accepted 26 Jan 2011; published 11 Feb 2011

3. The waveguide model of an ideal cone

The photoreceptors work as structures that guide light due to a difference in refractive index of the inner/outer segments and surrounding regions. Photoreceptor characteristics that influence the number of waveguide modes are the receptor diameter d_i, the index of refraction of the receptor n_i and the surrounding medium n_s, where the number of modes propagated are determined by the V-number. If $V < 2.405$ only the fundamental mode LP_{01} (Gaussian-like mode) is excited in the photoreceptor, otherwise higher-order modes differing from a Gaussian can be coupled.

According to the model of Snyder and Pask [8], the coupling of light incident to discrete modes propagating in the photoreceptor creates a directionality mechanism corresponding to an apodization effect at the pupil, where the apodization is assumed to be a linear combination of single-cone responses. The coupling efficiency in an individual photoreceptor is governed by the total power coupled to the modes allowed by the receptor, given by [9]:

$$P_{total}(\theta,\lambda) = \sum_{m=0}^{M} \left| \int\int E exp\left(\frac{i2\pi n_{eye}\theta x}{\lambda}\right) \psi_m^* dxdy \right|^2 \quad (1)$$

where E is the amplitude of the incident field, n_{eye} is the refractive index of the eye model, ψ_m is the normalized mode field amplitude, M is the number of modes allowed by the photoreceptor and θ is the angle of the light incidence. The coupling efficiency can be converted to the corresponding apodization effect at the pupil using $\theta = r_p / f_{eye}$ where $f_{eye} = 22.2mm$ and r_p is the pupil position.

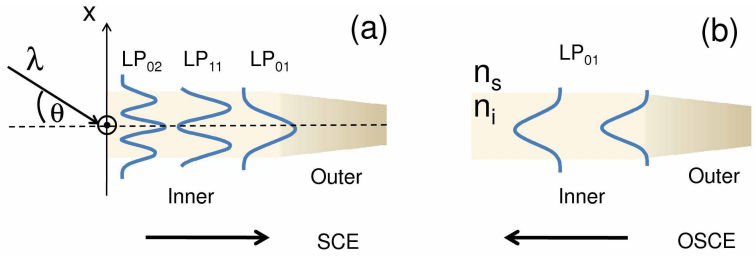

Fig. 3. Optical excitation of the retinal cone photoreceptor [9]: (a) from the inner to the outer segment for the SCE case and (b) backward-propagating for the OSCE.

After the coupling of light, the excited mode fields propagate from the inner to the outer segment (SCE case), posteriourly part of the light is reflected within each cone photoreceptor by scattering processes such that the backward-propagating mode is excited (OSCE case). As the outer segment is narrow, it is expected that only the fundamental mode can be efficiently excited for the OSCE case [9]. Both situations, i.e., a multimodal (SCE) and a single-mode (OSCE), have been simulated with the LF-PCF as described in the next sections. Clearly, variations exist for real photoreceptors cones that deviate significantly from the simpler cylindrical geometry of the individual waveguides of the LF-PCF used in this work. Such variations will tend to smoothen out abrupt spectral changes and minute refractive index variations of each cone, but highlight the genuine appearance of the SCE and OSCE [9, 15].

4. Results

4.1. Numerical aperture and Simulated Stiles-Crawford relation ($V \propto NA$)

By exploiting the large thermo-optical coefficient of the Castor Oil, it is possible to decrease the index of refraction of the Castor Oil from 1.477 to 1.459 at 620nm in steps of 0.5×10^{-5}

#135685 - $15.00 USD Received 28 Sep 2010; revised 3 Dec 2010; accepted 26 Jan 2011; published 11 Feb 2011

with the temperature-controlled oven. Therefore, the waveguide parameter is given by:

$$V(T) = (\pi d_i/\lambda)\sqrt{n_{oil}^2(T) - n_{silica}^2} \tag{2}$$

where d_i is the liquid-filled hole diameter, n_{oil} is the index of refraction of the filtrated liquid and n_{silica} is the index of refraction corresponding to the surrounding medium. At λ = 620nm and a temperature of 25°C the oil-filled holes have multi-mode characteristics (V>2.405) with 7 higher-order modes propagating. Above 71°C the waveguide becomes single mode (V< 2.405) coupling only the fundamental mode LP_{01}. The results are summarized in Table 1. In Fig. 3(b) and 3(c) the mode patterns propagating are imaged at 25°C (multimode) and 73°C (single mode).

Table 1. Waveguide modes and SCC directionality at different temperatures (λ = 620nm)

Temp. (°C)	25	67	69	71	71.3	71.5	73
n_{Coil}	1.4734	1.4601	1.4595	1.4589	1.4588	1.4587	1.4583
V	7.006	2.824	2.477	2.072	1.9968	1.9184	1.566
$LP_{m,n}(modes)$	01,02,11,12, 21,31,41.	01,11	01,11	01	01	01	01
ρ^* (mm^{-2})	0.002	0.046	0.059	0.121	0.128	0.132	0.166

*Standard Deviation = 0.001.

As shown in Fig. 4(a), the apodization effect at the pupil plane is obtained in a range of temperatures from 25°C up to 73°C. The solid lines correspond to a theoretical fit using a Super Gaussian function [23] sensible to multimode characteristics (manuscript in preparation). Here this function is only introduced to facilitate the visualization of the apodization. By using the conventional Stiles-Crawford function $\eta = 10^{-\rho r^2}$, where ρ is the simulated directionality factor, it is possible to determine at different V values, the results of which are summarized in Table 1.

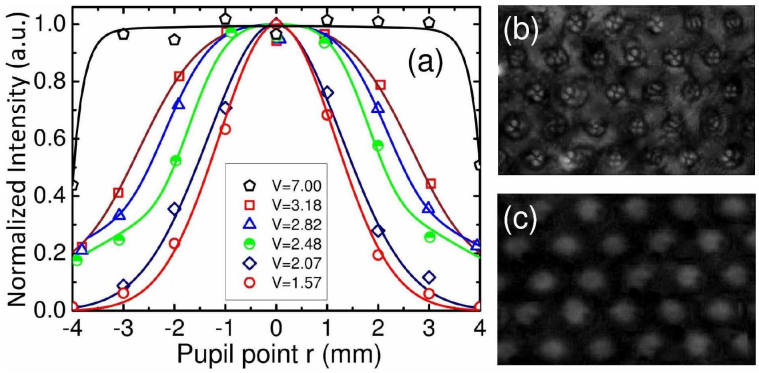

Fig. 4. (a) Experimentally determined pupil apodization effect at different waveguide parameters of the LF-PCF; section of fiber cladding: (b) multimode patterns at 25°C (V=7.00), and (c) single-mode at 73°C (V=1.57).

The measured directionality is highly sensitive to variations in refractive index, at 71°C a change of $\Delta n = 1 \times 10^{-4}$ (+0.3°C) corresponds to a change in the directionality factor of $\Delta\rho = 7 \times 10^{-3} mm^{-2}$. The sensitivity of the directionality factor to the exact values of refractive indices for the eye and retina has already been reported by Snyder and Pask [8], where

#135685 - $15.00 USD Received 28 Sep 2010; revised 3 Dec 2010; accepted 26 Jan 2011; published 11 Feb 2011

a small variation of $\Delta n = \pm 0.5\%$ can cause significant changes in the directionality results, a fact that is considered to challenge the waveguide model [11]. From our experimental results, an error value of $\Delta\rho \sim 5\%$ commonly reported in SCE experimental studies [6, 10, 24] corresponds to an error value in the step index function ($\delta n = n_i - n_s$) of $\Delta n \approx 6 \times 10^{-4}$. Note that the phase-contrast microscopy broadly used to measure refractive properties has a similar sensitivity to the refractive error as the SCE [25].

4.2. Spectral dependence of the Simulated Stiles-Crawford effect ($V \propto 1/\lambda$)

For the case of photoreceptors working as waveguides, due to the similitude in biological composition of the inner segments (pigments excluded) and the surrounding medium, it is expected that both have a similar dispersion. Therefore, across the visible spectrum the numerical aperture is approximately constant. In our experimental spectral simulations, the condition of a constant $NA(\lambda)$ is maintained in our spectral measurements by controlling the thermo-optical properties (for each wavelength). Furthermore, we have separated the nonspectral part of the Cutoff function defined as $A = \pi d_i NA$ and it is maintained a constant, such that V(λ)=A/λ.

4.2.1. Multi-mode characteristic of the simulated SCC-I

According to their geometry and refraction properties it is expected that foveal cones are single-mode in the red spectral region possibly becoming multimode at shorter wavelengths [8, 26]. Although the liquid-filled holes in the LF-PCF are larger than typical cone diameters reported for the fovea, a step-index refraction can be managed such that the V-number matches the expected average value for foveal cone photoreceptors. As shown in Fig. 5(a), the directionality factors are measured across the visible spectrum for different A values: (a) A=1.185μm, (b) A=1.326μm, (c) A=1.533μm.

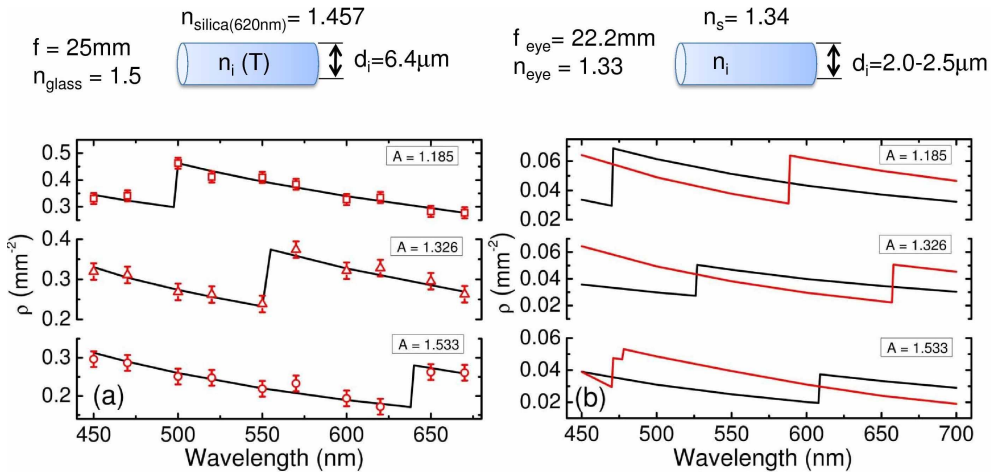

Fig. 5. (a) Wavelength dependence of the measured directionality for the LF-PCF (dots) and corresponding waveguide-model results [8] for different A values (A=1.185μm, 1.326μm, and 1.533μm). (b) Waveguide numerical results for photoreceptors of d_i=2.0μm (black line) and d_i=2.5μm (red line) using the same A values as the LF-PCF method. The numerical results shown are based on the above-indicated indices and dimensions.

The filled holes in the LF-PCF all have the same diameter, thus the spectral transitions are sharp when there are transitions in the number of modes allowed. For example, if A= 1.326μm and at wavelengths shorter than $\lambda \sim 555nm$, the waveguide parameter is larger than $V = 2.405$,

#135685 - $15.00 USD Received 28 Sep 2010; revised 3 Dec 2010; accepted 26 Jan 2011; published 11 Feb 2011

consequently new modes are coupled decreasing drastically the directionality value. The directionality values are well predicted by the waveguide model [Eq. (1)].

Following the same model it is possible to predict the directionality values expected for the foveal cones. As shown in Fig. 5(b), the wavelength dependence of the directionality factor is modelled for photoreceptors of diameter d_i=2.0μm (black line) and d_i=2.5μm (red line). We have used the refraction values of the surrounding medium as $n_s = 1.34$ [27] and different values for the refraction of the inner segment $n_i = 1.353$ [8], 1.356 and 1.363 [28] corresponding to A=1.185μm,1.326μm, and 1.533μm, respectively. The results resemble the values reported for the foveal results [10]. However, in the retinal mosaic the cones have small variations in diameter and composition, hence an overall contribution of the mosaic illuminated (usually Maxwellian illumination) would show smooth transitions between different modal regions when characterising the psycho-physical SCE [15].

4.2.2. Single-mode characteristic of the Simulated Optical Stiles-Crawford effect (OSCC)

As represented in Fig. 3, according to the model of light coupling to-and-from photoreceptors [9], predominantly the fundamental mode (LP_{01}) is excited by backscattered light such that the Gaussian apodization normally reported in OSCE studies is created by a single-mode characteristic of the waveguide.

Using the experimental method to simulate the OSCE equivalent case, the backscattered light coming from the interface oil-filled holes-air (analogue to outer segment scattering) is undetectable due to the background created by reflection at the first interfaces (air-glass and glass-oil). However, a single mode characteristic for the transmitted light of the LF-PCF can be satisfied throughout the spectral range via temperature tuning.

For the OSCC parameters, the temperature is controlled such that $V < 2.405$ (i.e. A = 1.08μm) can be satisfied from 450nm to 670nm. As shown in Fig. 6(a), the wavelength dependence of the directionality is in good agreement with the Snyder & Pask model [8] and the analytical model of B.Vohnsen et al. [9] given by:

$$\rho_{SOSC} = \log(e)\left(\frac{\pi n_{glass} w}{\lambda f}\right)^2 \tag{3}$$

where $n_{glass} = 1.5$ (glass plate), $f = 25mm$ (L_1) and $w = 3 \pm 0.2\mu m$ (hole radius) have been used.

In Fig. 6(b), the wavelength dependence of the directionality factor is modelled for photoreceptors whose size are d_i=2.0μm (black lines) and d_i=2.5μm (red lines). We have used the refraction values of the surrounding medium as $n_i = 1.34$ and 1.363 [28] and considered a single-mode contribution to the directionality factor. The wavelength dependence for the single-mode condition is in good agreement with the values reported by Zagers et al. for OSCE in 21 subjects [6]. Note that the inclusion of scattering from the combined illumination of many photoreceptors [5] is not a prerequisite to reproduce the wavelength dependence of the directionality factor.

5. Conclusion

We have demonstrated a liquid-filled photonic crystal fiber method to imitate the waveguide mechanism of individual cone photoreceptors and collectively simulate the retina. Its refractive properties are accurately managed by temperature allowing an accurate control of directionality characteristics and relating these to those of the human eye. The fiber-based photoreceptor simulator may be employed to study the impact of aberrations and light coherence under conditions that resemble vision [26].

#135685 - $15.00 USD Received 28 Sep 2010; revised 3 Dec 2010; accepted 26 Jan 2011; published 11 Feb 2011

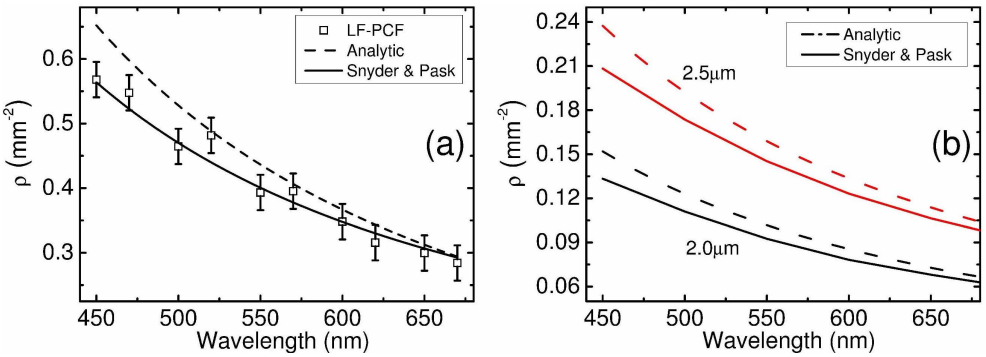

Fig. 6. (a) Wavelength dependence of the directionality obtained using the LF-PCF (dots) for the single-mode condition, A=1.08μm. (b) Waveguide numerical results for photoreceptors of d_i=2.0μm (black line) and d_i=2.5μm (red line). The numerical results correspond to the waveguide model (solid line) [8] and the analytical approximation (dotted curve) [9].

Acknowledgments

The authors wish to thank Rebeca B. Nunes for her help with the 3D image [Fig. 2(a)]. This research was supported by Science Foundation Ireland grants: 07/SK/B1239a and 08/IN.1/B2053.

#135685 - $15.00 USD Received 28 Sep 2010; revised 3 Dec 2010; accepted 26 Jan 2011; published 11 Feb 2011